

MODAL ANALYSIS AND EXPERIMENTAL STUDY ON THE WHITE-BODY OF A CRANE CAB

by

**De-Yuan ZONG^{a*}, Yang YU^a, Pei-Tao QIU^a,
San-Long WANG^b, and Jie YANG^a**

^a College of Civil Engineering, Xuzhou University of Technology, Xuzhou, Jiangsu, China

^b Jiangsu XCMG Construction Machinery Research Institute Co., Ltd., Xuzhou, Jiangsu, China

Original scientific paper

<https://doi.org/10.2298/TSCI2404581Z>

Taking a certain crane cab as the research object, firstly, according to the geometric model of the cab body-in-white, the finite element simulation model is established, and the finite element simulation modal calculation is carried out, and the first six natural frequencies and mode shapes of the cab simulation calculation are analyzed. The test natural frequency and modal shape of the body-in-white are obtained through the LMS data acquisition system, and the modal theory is used to analyze the modal correlation between the calculated mode and the experimental mode. Correctness is checked and verified. The results show that the finite element simulation model has high accuracy and can simulate the overall performance of the actual structure, which can provide real data for later product optimization.

Key words: *body in white, finite element simulation, crane cab, natural frequency, experimental mode*

Introduction

Construction machinery usually works in harsh environment and operates for a long time. The cab will vibrate due to the excitation of various vibration sources [1, 2]. To ensure the dynamic characteristics of the crane during driving and operation, it is of great significance to conduct structural modal calculation and inherent vibration analysis on the cab body in its original state, which will facilitate subsequent structural improvements for the cab.

Currently, the combination of finite element analysis and modal experiment is widely employed for efficient and rapid investigation of cab modal characteristics, providing a direct foundation for further structural optimization or research [3, 4].

Fundamental principles of modal analysis

The methods of modal analysis encompass both theoretical and experimental approaches. Theoretical modal analysis is based on the principles of linear vibration theory and is obtained through finite element simulation calculations. The process of experimental modal analysis involves parameter identification through the utilization of advanced testing and data acquisition technologies. In the initial stage of experimental modal analysis, theoretical modal calculations are necessary to determine the distribution and positioning of measurement points, while the results obtained from experimental modal analysis can be used to calibrate the theoretical modal calculations, thereby enhancing the accuracy of finite element simulation models.

* Corresponding author, e-mail: 332306181@qq.com

The crane cab system can be approximated as a multi-degree-of-freedom linear system, and its kinematic differential equation is expressed:

$$M\ddot{y}(t) + C\dot{y}(t) + Ky(t) = x(t) \quad (1)$$

where M is the mass matrix, C – the damping matrix, K – the stiffness matrix, $\ddot{y}(t)$ – the vibration acceleration, $\dot{y}(t)$ – the velocity, $y(t)$ – the displacement, and $x(t)$ – the excitation of the system.

By employing simplification, the cab body in white applies the vibration theory of a single degree of freedom system to address the dynamics problem, disregarding damping forces in calculations. The solution is presented:

$$M\ddot{y}(t) + Ky(t) = 0 \quad (2)$$

According to the theory of vibration, the free oscillation of any elastic body can be decomposed into a superposition of simple harmonic vibrations. The displacement variation follows a sine function can be given:

$$y(t) = Y \sin(\omega t) \quad (3)$$

where $y(t)$ is the displacement, Y – the amplitude, and t – the stands for time.

Employ eqs. (3) and (2) and facilitate the solution process:

$$K - \omega^2 My(t) = 0 \quad (4)$$

where the eigenvalues of the vibration equation, which are essentially the roots of the characteristic equation $\omega_i (i = 1, 2, 3, \dots, n)$ can be obtained through solving eq. (4). Subsequently, one can derive both the modal natural frequency and vibration mode [5].

The crane cab is a complex system with multiple degrees of freedom, exhibiting an infinite number of modes and natural frequencies. Therefore, when investigating the system response of cab BIW, only the low order natural frequencies that exert a significant influence on the vibration system and their corresponding modes are selectively extracted.

Theory of modal pattern correlation analysis

The research methodology employed in this study involves the integration of theoretical modal analysis and experimental modal analysis to examine the dynamic characteristics of the structure. The inner product correlation method enables the determination of the correlation and reliability between experimental modal analysis and theoretical simulation calculations.

For a linear system with multiple degrees of freedom, let R^n denote an n -dimensional real linear space. The value of $X = \{x_1, x_2, \dots, x_n\}$, $X \in R^n$ is the test vibration mode of the experimental mode, $Y = \{y_1, y_2, \dots, y_n\}$. The mode shape $Y \in R^n$ represents the calculated mode, while the inner product is defined:

$$\langle X, Y \rangle = \sum_{k=1}^n x_k y_k$$

and the correlation based on inner product

$$C_p(X, Y) = \frac{|\langle X, Y \rangle|}{\sqrt{\langle X, X \rangle \langle Y, Y \rangle}}$$

is demonstrable $0 \leq C_p \leq 1$. The closer the value of $C_p(X, Y)$ Approaches 1, the higher the credibility and agreement between the computational model and experimental data are presented in [6, 7].

Finite element modelling and model analysis of the cab

According to the existing cab BIW geometry model, the grid partition was subsequently performed, resulting in the generation of the finite element model for cab BIW, as depicted in fig. 1.

Table 1 presents the first six orders of free mode frequency and corresponding vibration modes.

Table 1. Simulation-based calculation of cab modal outcomes

Order	Frequency	Vibrational mode
1	23.403	First-order bending of the ceiling
2	23.995	A whole twist
3	32.258	First-order flexure of the lower plate
4	36.845	Two-step bending of the ceiling
5	38.128	Mixed vibration of floor and side panels
6	41.200	Mixed vibration of floor and side panels

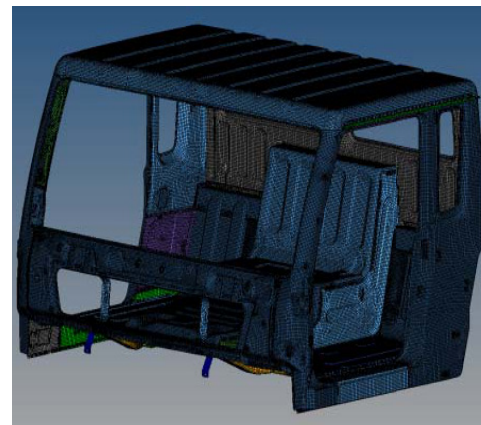


Figure 1. Finite element model for cab body-in-white simulation

According to the first six orders of simulation modal results, in conjunction with the actual operational conditions of the cab, particular attention is given to the first order modal modes, as depicted in fig. 2.

The first-order mode calculated is the bending vibration mode of the ceiling at a frequency of 23.403 Hz, with the primary deformation occurring in the cab's ceiling. The occurrence of first-order modal vibration in the cab may result in fatigue strength failure of the ceiling. The stiffness of the ceiling center area necessitates reinforcement measures. Considering both practicality and cost-effectiveness, it is advisable to incorporate additional reinforcement bars or welding points into the ceiling structure for improved rigidity.

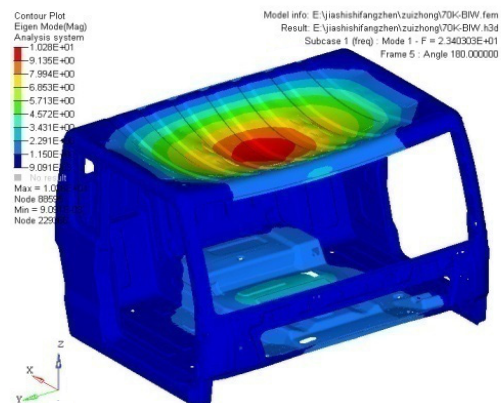


Figure 2. Simulation calculation of first order vibration mode for BIW (23.403 Hz)

Modal experiment on cab transportation

Conduct a modal test on the unpainted cab body to validate the accuracy of the simulation calculations and refine the model if necessary. The selection of test detection points necessitated an even distribution while reflecting the geometric characteristics of the structure. A total of 151 detection points were chosen for the BIW test, with the distribution of cab detection points illustrated in fig. 3.

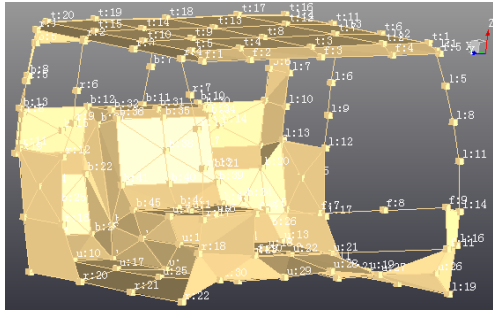


Figure 3. Response point of the cab body-in-white

The selection of excitation points avoids vibration nodes, structural weak points, and suspension points to ensure optimal results. Additionally, the shaker's convenient installation facilitates easy transmission of the excitation force to various parts of the structure.

The arrangement of the shakers can be observed in fig. 4. Response measurement points were assessed in batches, and the resulting data was subjected to analysis. The frequency, damping statistics, and mode description were focused on the 0-200 Hz range and limited to the first six order modes, as presented in tab. 2.



Figure 4. Reconfiguration of Shaker 1 for Installation

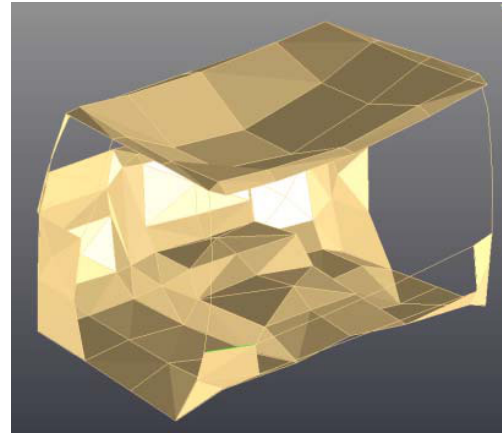


Figure 5. First -order vibration mode experiment of body in white (23.432 Hz)

Table 2. Description of the first six order frequencies, damping, and mode shapes in the test data

Order	Frequency [Hz]	Damping ratio [%]	Description of vibration modes
1	23.432	1.50	First-order bending of the ceiling
2	23.858	0.70	A whole twist
3	31.640	0.52	First-order bending of the bottom plate
4	35.746	1.29	Two-step bending of the ceiling
5	37.971	0.41	Mixed vibration of floor and side panels
6	41.503	0.75	Mixed vibration of floor and side panels

According to the simulation results, particular attention is given to the first-order modes, as depicted in fig. 5.

According to the experimental modal analysis results, the first six orders of natural vibration frequencies of the cab range from 20-50 Hz. The predominant deformation in the vibration modes is primarily observed in the ceiling, floor, and side panels. The initial ten modes of the entire body predominantly exhibit local ceiling modes. In the event of resonance, vibrations generate noise, thereby diminishing the driver's ride comfort.

Correlation analysis of modal shapes

The present study evaluates the quality of modal testing and verifies the accuracy of the finite element model through a correlation analysis between simulated and experimental modal frequencies. The results depicted in fig. 6 demonstrate that the majority of values within the frequency range of 0-100 Hz exceed 0.9, with only a small number of peak values falling below this threshold. Furthermore, most values tend to approach unity. Consequently, the simulation calculation model for cab BIW exhibits a remarkable level of concordance with the experimental model's dynamic characteristics and can be deemed highly reliable. It implies that the cab BIW simulation model is valid and effectively captures the dynamic characteristics of the physical structure.

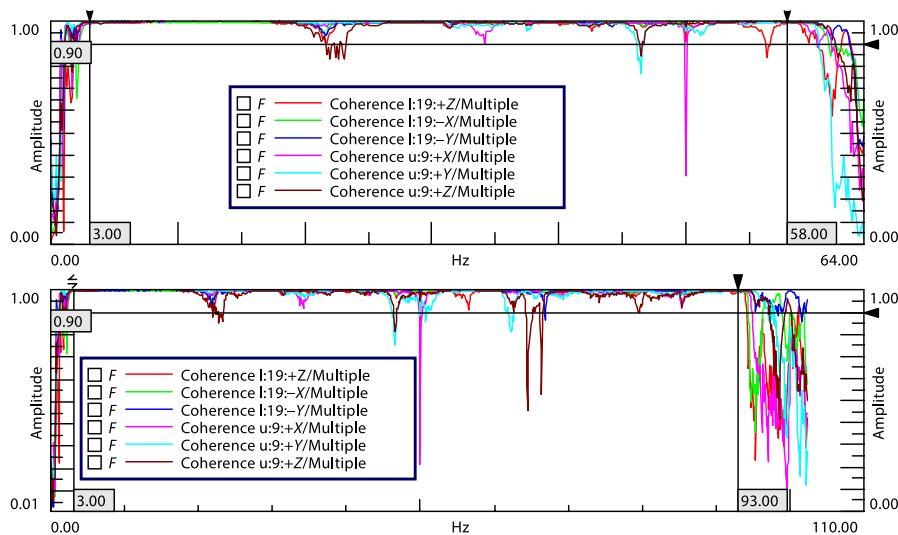


Figure 6. Coherent coefficients corresponding to the frequency response function

Conclusion

The geometric model of the cab body in white is simplified in this paper, and a finite element simulation model is established. Subsequently, the first six free modes are computed, followed by conducting modal analysis for structural simulation. Finally, the objective analysis of the correlation between the finite element model and the experimental model is conducted using mode correlation analysis theory. This suggests that the simulation model accurately captures the dynamic characteristics of the actual structure, making it a reliable foundation for enhancing cab structural design.

References

- [1] Chen, S., et al., Interior Noise Prediction and Analysis of Heavy Commercial Vehicle Cab, *SAE Paper*, 1 (2011), 2241

- [2] Kim, K. C., *et al.*, Process of Designing Body Structures for the Reduction of Rear Seat Noise in Passenger Car, *International Journal of Automotive Technology*, 8 (2007), 1, pp. 67-73
- [3] Zhu, M. T., *et al.*, Modal Testing and Analysis of Body in White for Mini Cars, *Journal of Chongqing Jiaotong University (Natural Science)*, 29 (2010), 4, pp. 659-662
- [4] Tianfei. M. A., *et al.*, Modal Analysis and Experimental Study of Cab Body in White, *Automotive Engineering*, 31 (2009), 7, pp. 616-619
- [5] Zou, X. H., *et al.*, Vibration Characteristics Analysis of Light Truck Axle Housing, *Journal of Chongqing University of Technology (Natural Science)*, 31 (2017), 12, pp. 1-7
- [6] Cao, Q. Y., *et al.*, Modal Correlation Analysis Utilizing Inner Product, *Chinese Journal of Applied Mechanics*, 12 (1998), 2, pp. 135-138
- [7] Zhai, X., *et al.*, Enhanced Technology Employing Uncorrelated Mode Modulation, *Journal of Aerospace Power*, 2 (2017), 1, pp. 405-415